A Temperature-Dependent Model for Ultimate Bearing Capacity of Energy Piles in Unsaturated Fine-Grained Soils

Sannith Kumar Thota, A.M.ASCE[1]; Farshid Vahedifard, F.ASCE[2]; and John S. McCartney, F.ASCE[3]

Abstract: This study presents an analytical framework to estimate the change in ultimate bearing capacity of energy piles in unsaturated fine-grained soils under drained mechanical loading conditions after drained heating. The framework was developed by extending conventional methods for the ultimate bearing capacity of piles in unsaturated soils to temperature-dependent conditions, where thermally induced changes in the characteristics of the unsaturated soil and soil–pile interface are considered. Specifically, the thermally induced variations in matric suction and effective saturation profiles with depth were incorporated into calculations of the shaft capacity and the end bearing capacity of piles in unsaturated soils. The proposed ultimate bearing capacity model is validated against experimental data for an energy pile loaded to failure in unsaturated Bonny silt, and a good match between measured and predicted values was obtained. A parametric study was carried out to evaluate the effects of infiltration rate and pile aspect ratio (i.e., pile embedment length/pile diameter) on the ultimate bearing capacity of energy piles in unsaturated clay and silt layers subjected to temperatures ranging from 5°C to 45°C. For both soils, the shaft, end bearing, and ultimate bearing capacities vary with an increase in temperature. At the reference temperature, the shaft, end, and ultimate bearing capacities vary monotonically with pile embedment length, while at elevated temperatures they vary nonmonotonically with pile embedment depth. At a given temperature, the parametric study shows that the bearing capacity of energy piles in clay decreases with increasing downward infiltration of water into the soil profile surrounding the energy pile, while in silt it may decrease or increase depending on pile embedment length. The ultimate bearing capacity increases with a decrease in pile aspect ratio at all temperatures. Estimates of the ultimate bearing capacity of energy piles in unsaturated fine-grained soils from the framework are a critical part of thermomechanical soil–structure interaction analyses needed to design energy piles, so this study contributes toward the widespread application of this emerging technology in practice.
DOI: 10.1061/(ASCE)GT.1943-5606.0002676.

Author keywords: Unsaturated soils; Energy piles; Bearing capacity; Temperature; Fine-grained soils.

Introduction

Deep foundations are extensively used in various geotechnical and geoenvironmental applications to transfer mechanical loads to firm strata, resist horizontal and uplift movements, and minimize settlements. Estimating the ultimate bearing capacity of a deep foundation is an important step in their geostructural design. Most methods used in practice for estimating the ultimate bearing capacity of deep foundations are focused on saturated soils (e.g., Skempton 1959; Chandler 1968; Burland 1973), and only in the past two decades have studies focused on the behavior of deep foundations in unsaturated soil layers. For instance, Georgiadis et al. (2003) used finite-element analysis to study the influence of unsaturated soil conditions on the behavior of piles, while Vanapalli and Taylan (2012) extended methods originally developed for saturated soils to unsaturated soils under both drained and undrained mechanical loading.

Over the past decade, there has been a rapidly growing interest toward integrating geothermal heat exchangers into deep foundations to improve the efficiency of heating and cooling systems for buildings (e.g., Brandl 2006; Laloui et al. 2006; Loveridge et al. 2019; McCartney et al. 2019; Laloui and Loria 2019). During heat exchange operations, the temperature of these piles (referred to as energy piles) typically varies between 5°C and 35°C (e.g., McCartney and Murphy 2017), although some laboratory studies have evaluated the effects of temperatures as high as 45°C (Xiao et al. 2014; Liu et al. 2019; Goode and McCartney 2015). In energy piles, axial stresses may be induced by heating that are superimposed atop the axial stresses due to mechanical loading. Although it is desirable for the combined thermomechanical stresses to be within the elastic range, the temperature changes can affect the soil surrounding the pile and, in turn, affect the ultimate bearing capacity. The majority of previous studies on the ultimate bearing capacity of energy piles are limited to dry or saturated conditions (Kramer and Basu 2014; Wang et al. 2015; Ng et al. 2015; Loria et al. 2015; Goode and McCartney 2015) and fewer studies have focused on unsaturated conditions (Uchaipichat 2005, 2012, 2013; McCartney and Rosenberg 2011; Goode and McCartney 2015; Akrouch et al. 2016). Knowledge of the ultimate bearing capacity of energy piles is critical in thermomechanical load transfer (T-z) analyses, so understanding the impact of unsaturated conditions on the components of the ultimate bearing capacity will lead to improved designs considering soil–structure interaction (e.g., Knellwolf et al. 2011; Chen and McCartney 2016). Gaps remain for an analytical framework that can reasonably capture the

[1]Senior Staff Engineer, Schnabel Engineering, 46020 Manekin Plaza #150, Sterling, VA 20166; formerly, Ph.D. Candidate, Richard A. Rula School of Civil and Environmental Engineering, Mississippi State Univ., Mississippi State, MS 39762. Email: sannyy21@gmail.com

[2]CEE Advisory Board Endowed Professor and Professor, Richard A. Rula School of Civil and Environmental Engineering, Mississippi State Univ., Mississippi State, MS 39762 (corresponding author). ORCID: https://orcid.org/0000-0001-8883-4533. Email: farshid@cee.msstate.edu

[3]Professor and Department Chair, Dept. of Structural Engineering, Univ. of California, San Diego, La Jolla, CA 92093-0085. ORCID: https://orcid.org/0000-0003-2109-0378. Email: mccartney@ucsd.edu

Note. This manuscript was submitted on October 23, 2020; approved on July 20, 2021; published online on September 13, 2021. Discussion period open until February 13, 2022; separate discussions must be submitted for individual papers. This paper is part of the ***Journal of Geotechnical and Geoenvironmental Engineering***, © ASCE, ISSN 1090-0241.

effects of temperature on the ultimate bearing capacity of energy piles in unsaturated soils.

This study aims to provide insight into the effects of temperature and unsaturated conditions on the ultimate bearing capacity of energy piles with a practical goal of facilitating the computationally efficient design and analysis of energy piles in unsaturated soils. For this purpose, this paper presents an analytical framework built on fundamental theories to estimate the ultimate bearing capacity of energy piles in unsaturated soils subject to varying temperatures under drained heating and mechanical loading conditions. A temperature-dependent model for effective stress is incorporated into the formulation of the shaft and end bearing capacity of the energy pile. The proposed model includes the effect of temperature on matric suction, degree of saturation, and pile–soil interface strength. The model is validated against data available in the literature. A parametric study is carried out to evaluate the effects of flow rate and aspect ratio (i.e., pile embedment length/pile diameter) on the ultimate bearing capacity of an energy pile in clay and silt at temperatures ranging from 5°C to 45°C.

Background

The ultimate bearing capacity of an energy pile is expected to vary during drained heating due to the effects of temperature on the properties of the soil, pile, and soil–pile interface. Results of tests in the literature report different trends of ultimate bearing capacity of energy piles with temperature. McCartney and Rosenberg (2011) observed a 40% increase in the ultimate capacity of an energy pile in unsaturated Bonny silt after heating the pile in the centrifuge by 41°C. However, they did not characterize the changes in water content of the soil surrounding the energy pile during heating. Wang et al. (2015) tested a pile in silt at 1 g and found that the ultimate capacity of the pile at 38°C was higher than that at 20°C. Ng et al. (2015) performed centrifuge tests on energy piles in saturated sand and found that an increase in ultimate bearing capacity of 13% occurred primarily due to changes in shaft capacity when the pile was heated from 22°C to 37°C. However, they observed that a larger increase in ultimate bearing capacity of 30% occurred primarily due to changes in end bearing capacity when the pile was heated from 22°C to 52°C. Many investigators have developed semianalytical or numerical models to study the effect of temperature on soil–structure interaction, although most did not consider the effect of temperature on the bearing capacity (e.g., Knellwolf et al. 2011; Suryatriyastuti et al. 2013, 2014; Olgun et al. 2015; Saggu and Chakraborty 2015; Chen and McCartney 2017). Further, other studies have compared results from numerical simulations with thermal stress and strain data from heating tests on full-scale energy piles (e.g., Di Donna and Laloui 2013; Di Donna et al. 2016b; Loria et al. 2015; Fuentes et al. 2016; Fu 2017). Several of these studies have found that an increase in temperature leads to increases in the magnitude of the shaft and end bearing capacities of the pile.

The effect of temperature on the properties of the soil–energy pile interface is another factor that can influence the ultimate bearing capacity of energy piles. Akrouch et al. (2014) and Yavari et al. (2016) reported negligible changes in the interface friction angle and adhesion of soil–pile interfaces. Murphy and McCartney (2014) performed borehole shear tests with heated concrete interface pads and found negligible changes in interface friction angle with temperature. Di Donna et al. (2016a) conducted tests on saturated clay–concrete interfaces at different temperatures and found an increase in the apparent adhesion and a reduction in interface friction angle during heating. Fu (2017) observed that an increase in temperature can cause a decrease in water content and an increase in the interface friction angle and adhesion for interfaces between concrete and unsaturated soil. Yazdani et al. (2019) performed a set of laboratory tests and found that the shear strength of a saturated clay–concrete pile interface increases with temperatures from 24°C to 34°C, possibly due to changes in clay volume at the interface. Vasilescu et al. (2019) observed only small changes in the interface friction angle (i.e., within 0.7°) for a saturated soil–concrete pile interface sheared at temperatures of 8°C, 13°C, and 18°C.

There are very few studies that have investigated energy piles under unsaturated conditions. However, existing studies show that the overall performance of energy piles is affected by the unsaturated conditions and temperatures (e.g., McCartney and Rosenberg 2011; Goode and McCartney 2015; Wang et al. 2012; Uchaipichat 2013; Akrouch et al. 2014; Fu 2017; Behbehani and McCartney 2020a, b; Thota and Vahedifard 2020). Wang et al. (2012) reported a reduction in the shaft capacity of a pile in fine sand with initial gravimetric water contents of 0%, 2%, and 4% when the pile temperature was increased from 20°C to 60°C, although they studied an aluminum energy pile that may have mobilized a fraction of the ultimate capacity during heating prior to mechanical loading. Goode and McCartney (2015) performed centrifuge tests on a model thermoactive pile embedded in silt. They observed a decrease in water content and an increase in pile shaft capacity because of heating the pile from room temperature to 41°C. Behbehani and McCartney (2020a) used a coupled thermo-hydro-mechanical model to explain that this increase in capacity was due to thermally induced drying of the surrounding soil during monotonic heating, which led to an increase in effective stress and shear strength. Behbehani and McCartney (2020b) used this model to study the seasonal cyclic heating and cooling response of energy piles and found only minor changes in degree of saturation with time, indicating that drained conditions can be assumed. Coupled heat transfer and water flow models may provide the best interpretation of the transient processes in unsaturated soils surrounding energy piles, but simplified analytical approaches are preferred for energy pile design.

Model Development

Conceptual Model of Ultimate Bearing Capacity of Piles under Varying Temperatures

Proper design of energy piles warrants a careful examination of all parameters that are affected by changes in hydraulic and mechanical loads under varying temperatures. In this study, the ultimate bearing capacity of an energy pile in an unsaturated soil layer is determined by quantifying the shaft and end bearing capacities under varying degrees of saturation and temperatures. The effects of degree of saturation (or suction) and temperature are accounted for in the properties of the surrounding unsaturated soil, as well as the soil–pile interface under drained mechanical loading conditions. The temperature distribution within the pile is assumed to be constant and heating is assumed to be drained (i.e., all thermal volume changes in the soil have occurred and there are no excess pore water pressures or changes in degree of saturation). These assumptions can reasonably represent field conditions in which the changes in the average temperature of the energy pile occur slowly over several months and sufficient time is permitted for dissipation of pore water pressures (Behbehani and McCartney 2020b). For these conditions, it can also be assumed that the soil surrounding the energy pile reaches an almost constant temperature along the pile length. Several studies including field and laboratory tests observed constant soil temperatures

along the length of the pile (e.g., Laloui et al. 2006; Bourne-Webb et al. 2009; Kalantidou et al. 2012; Murphy et al. 2015; Ng et al. 2015; McCartney and Murphy 2017; Vasilescu et al. 2019; Elzeiny et al. 2020). Increases in pile dimensions due to thermal expansion are not considered. Several studies (e.g., Knellwolf et al. 2011; Chen and McCartney 2017) have shown that thermally induced changes in the pile dimensions are small enough that they do not result in significant changes in radial stress and side shear restraint. Further, the change in length of the energy pile is not significant enough to change the area used in the calculation of the shaft capacity.

The pile temperature affects the effective stress and apparent cohesion in the soil through thermal changes in the matric suction and degree of saturation, which in turn alter the ultimate bearing capacity of the pile. The magnitude of thermally induced variation in the ultimate bearing capacity of an energy pile depends on the soil type and pile embedment depth. Triggered by changes in hydraulic properties and apparent cohesion, thermally induced changes in the pile–soil interface strength can also affect the ultimate bearing capacity. At the edge of the pile, the thermally induced water flow in unsaturated soils occurs due to several phenomena arising from temperature effects on water properties (density, viscosity, surface tension, etc.), soil-water retention properties, and vapor diffusion (Philip and De Vries 1957; Grant 2003; Başer et al. 2018; Behbehani and McCartney 2020a, b; Thota 2020). These factors together cause water to flow through the soil away from the pile, leading to desaturation, which in turn can affect the thermal efficiency of the energy pile (e.g., Akrouch et al. 2016). This is mainly due to the lower thermal conductivity of dry and unsaturated soils compared to saturated soils (Campbell et al. 1994; Lu and Dong 2015). This study attempts to develop a framework to investigate the effect of changes in hydraulic profiles with drained heating and their impact on the ultimate bearing capacity of piles under drained mechanical loading. This is achieved by considering the effect of temperature on the suction profile through a combination of water retention mechanisms and water properties with Darcy's law. For simplicity and to avoid complex coupled mass and energy analyses, this study ignores the effect of thermally induced vapor diffusion and phase change on the ultimate bearing capacity of energy piles. Heat transfer was also not considered in the model, and it was assumed that the pile and soil at the pile–soil interface were at equilibrium under an applied value.

Drained Heating

The shear strength and bearing capacity of unsaturated soils are mainly controlled by changes in matric suction and degree of saturation. Thus, the first step toward developing the temperature-dependent formulation for the ultimate bearing capacity involves the determination of matric suction and degree of saturation profiles under drained heating conditions. Building upon the effective stress principle of Bishop (1959), the suction stress–based effective stress of unsaturated soils was defined by Lu et al. (2010) as

$$\sigma' = (\sigma - u_a - \sigma^s) \tag{1}$$

where σ = total stress; u_a = pore-air pressure; and σ^s = suction stress, which can be represented as (Lu et al. 2010)

$$\sigma^s = -\psi S_e \tag{2}$$

where ψ = matric suction; and S_e = effective degree of saturation. The suction stress can be used to estimate the shear strength of unsaturated soils using the Mohr-Coulomb failure criteria as follows (Lu et al. 2010; Vahedifard et al. 2016)

$$\tau = c' + (\sigma - u_a - \sigma^s)\tan\phi' \tag{3}$$

where τ = shear strength; c' = effective cohesion arising from cementation; and ϕ' = effective friction angle. The aforementioned formulations [Eqs. (1)–(3)], which were originally defined under ambient temperature conditions, can be extended to temperature-dependent conditions by incorporating temperature-dependent matric suction and the soil-water retention curve (SWRC) (Vahedifard et al. 2018, 2019). The impact of temperature on the matric suction can be expressed as follows (Grant and Salehzadeh 1996):

$$\psi = \psi_{T_r}\left(\frac{\beta + T}{\beta_{T_r} + T_r}\right) \tag{4}$$

where ψ_{T_r} = matric suction at the reference temperature T_r. As defined, β_{T_r} is a regression parameter at the reference temperature, which depends on surface tension, enthalpy of immersion per unit area, and contact angle. The parameter β is calculated as (Grant and Salehzadeh 1996)

$$\beta = \frac{-\Delta h T_r}{-\Delta h + a(\cos\alpha')_{T_r} + b(\cos\alpha')_{T_r} T_r} \tag{5}$$

where α' = temperature-dependent soil-water contact angle; a and b = fitting parameters that can be estimated as $a = 0.11766\ \text{N} \cdot \text{m}^{-1}$ and $b = -0.0001535\ \text{N} \cdot \text{m}^{-1}\,\text{K}^{-1}$ (Dorsey 1940; Haar et al. 1984); and Δh = enthalpy of immersion per unit area, which can be determined by experimental measurements or by using the differential enthalpy of adsorption of the vapor (Vahedifard et al. 2020). Grant and Salehzadeh (1996) neglected the effect of temperature on the enthalpy of immersion even though Watson (1943) demonstrated that temperature could affect the enthalpy of immersion as well. In this study, as suggested by Vahedifard et al. (2018, 2019), the following temperature-dependent equation of Watson (1943) is used to define the enthalpy of immersion per unit area:

$$\Delta h = \Delta h_{T_r}\left(\frac{1 - T_r}{1 - T}\right)^{0.38} \tag{6}$$

where Δh_{T_r} = enthalpy of immersion per unit area at the reference temperature.

The temperature-dependent form of the soil-water contact angle is given as (Grant and Salehzadeh 1996)

$$\cos\alpha = \frac{-\Delta h + TC_1}{a + bT} \tag{7}$$

where C_1 is a constant, which can be determined as (Grant and Salehzadeh 1996)

$$C_1 = \frac{\Delta h_{T_r} + a(\cos\alpha)_{T_r} + b(\cos\alpha)_{T_r} T_r}{T_r} \tag{8}$$

The regression parameters and the aforementioned equations are thoroughly discussed and validated in Vahedifard et al. (2018, 2019).

Using the Brooks and Corey (1964) SWRC model and the temperature-dependent matric suction, the temperature-dependent effective saturation can be written as (Vahedifard et al. 2018, 2019)

$$S_e = \left(\frac{\psi_{aev}}{\psi\left(\frac{\beta_{T_r} + T_r}{\beta + T}\right)}\right)^{n_{BC}} \tag{9}$$

where ψ_{aev} and n_{BC} = fitting parameters representing the air entry parameter and pore size distribution parameter of the SWRC, respectively.

The temperature-dependent hydraulic conductivity can be described by employing the Gardner (1958) hydraulic conductivity function (HCF)

$$k = k_s e^{-\psi_{aev} \times \psi} \tag{10}$$

where k = hydraulic conductivity; and k_s = hydraulic conductivity of saturated soil. Eq. (10) considers the changes in soil hydraulic conductivity with temperature-dependent matric suction [Eq. (4)]. In addition to its effect on matric suction, temperature affects the hydraulic conductivity in Eq. (10) through thermally induced changes in the hydraulic conductivity of saturated soil. Specifically, k_s is inversely related to the water viscosity, which depends on temperature (Pillsbury 1950; Philip 1969). The relationship between the hydraulic conductivity of saturated soil and temperature can be defined by Constantz (1982)

$$k_s = \frac{k_{in}\gamma_w}{\eta(T)} \tag{11}$$

where k_{in} = intrinsic permeability assumed to be dependent only on the soil; γ_w = unit weight of water; and $\eta(T)$ = water viscosity. The water viscosity varies with temperature as follows (Lide 1995):

$$\eta(T) = 0.0002601 + 0.001517 \exp[-0.034688 \times (T - 273)] \tag{12}$$

The temperature-dependent equations for matric suction [Eq. (4)], effective saturation [Eq. (9)], and hydraulic conductivity [Eq. (10)] can be used along with a flow analysis to estimate the depth profiles of matric suction and degree of saturation for different water table depths and flow rates. For one-dimensional vertical liquid water flow in isotropic and homogenous materials, Darcy's law is given as follows:

$$q = -k\left(\frac{1}{\gamma_w}\frac{d\psi}{dz} + 1\right) \tag{13}$$

where z = distance above the water table; and q = steady vertical fluid flow rate (zero for hydrostatic, negative for infiltration, and positive for evaporation). Extending upon the analytical solution developed by Lu and Griffiths (2004), the one-dimensional suction profiles in unsaturated soil layers for different temperatures and infiltration rates can be defined as (Thota et al. 2019; Thota and Vahedifard 2021)

$$\psi = \frac{\gamma_w}{\psi_{\text{aev}}} \ln\left[\left(1 + \frac{q}{k_s}\right)e^{-\psi_{aev} z} - \frac{q}{k_s}\right]\left(\frac{\beta_{T_r} + T_r}{\beta + T}\right) \tag{14}$$

Using the SWRC model of Brooks and Corey (1964) and the HCF of Gardner (1958), the temperature-dependent effective saturation profile with depth can be written as (Thota et al. 2019; Thota and Vahedifard 2021)

$$S_e = \left\{\exp\left[\ln\left(\left(1 + \frac{q}{k_s}\right)e^{-\psi_{aev} z} - \frac{q}{k_s}\right)\left(\frac{\beta_{T_r} + T_r}{\beta + T}\right)\right]\right\}^{1/n_{BC}} \tag{15}$$

Mechanical Loading

The ultimate bearing capacity of energy piles in unsaturated soils is generally assumed to be comprised of two components, the shaft capacity and the end bearing capacity, and is given by

$$Q_{(\text{unsat})} = Q_{s(\text{unsat})} + Q_{e(\text{unsat})} \tag{16}$$

where $Q_{(\text{unsat})}$ = ultimate bearing capacity of the pile; $Q_{s(\text{unsat})}$ = shaft capacity; and $Q_{e(\text{unsat})}$ = end bearing capacity.

An energy pile is subjected to varying temperatures combined with mechanical loading during its operation. In this section, the temperature-dependent hydraulic formulations discussed in the previous section are employed to extend the ultimate bearing capacity formulations at ambient conditions to temperature-dependent conditions, to estimate the temperature-dependent ultimate bearing capacity. Under drained mechanical loading, the shaft capacity of a pile with length (L) and diameter (D) embedded in unsaturated soil under ambient temperature is given by

$$Q_{s(\text{unsat})} = [c'_a + \beta_c(\sigma - u_a + \psi S_e)]\pi DL \tag{17}$$

where c'_a = adhesion component of the interface shear strength for saturated conditions (typically equal to zero unless the soil is cemented); β_c = Burland-Bjerrum coefficient that can account for the installation method; and $(\sigma - u_a)$ = net normal stress. Unlike previous models for piles in unsaturated soils (e.g., Vanapalli and Taylan 2012), Eq. (17) uses the effective saturation instead of the degree of saturation and has fewer parameters.

Extending Terzaghi's bearing capacity equation to unsaturated conditions, assuming no surcharge, the end bearing capacity of unsaturated soils under drained mechanical loading conditions is written as

$$Q_{e(\text{unsat})} = [N_c(\sigma - u_a + \psi S_e)]\frac{\pi D^2}{4} \tag{18}$$

The ultimate bearing capacity of piles in unsaturated soils under drained mechanical loading is given by

$$Q_{(\text{unsat})} = [c'_a + \beta_c(\sigma - u_a + \psi S_e)]\pi DL + [N_c(\sigma - u_a + \psi S_e)]\frac{\pi D^2}{4} \tag{19}$$

Eq. (19) can be used to estimate the ultimate bearing capacity of an energy pile in unsaturated soil at ambient temperature conditions and can consider different cases where the suction and effective saturation vary with depth. In the end bearing capacity term in Eq. (19), the matric suction and effective saturation values correspond to the tip of the pile. In this study, Eq. (19) was extended to account for the effects of temperature on the degree of saturation and matric suction, which affect the effective stress. In other words, the degree of saturation decreases at the pile–soil interface due to thermally induced water flow away from the interface, the matric suction increases, and the degree of saturation decreases (Goode and McCartney 2015; Fu 2017). Therefore, the changes in the shear strength of the pile–soil interface can be captured by incorporating thermally induced changes in the SWRC, apparent cohesion (stemming from matric suction), and effective stress. The temperature dependency of pile–soil interface strength can be defined as follows:

$$\tau_T = (\sigma - u_a)\tan\delta' + c'_a + c_{\text{app},T} \tag{20}$$

$$c_{\text{app},T} = -\sigma^s \tan\delta' \tag{21}$$

where τ_T = interface shear strength; and $c_{\text{app},T}$ = apparent cohesion, which can be defined as a function of depth and temperature as follows:

$$c_{\text{app},T} = \tan\delta' \left\{ \exp\left[\ln\left(\left(1+\frac{q}{k_s}\right) e^{-\psi_{\text{aev}} z} - \frac{q}{k_s} \right) \left(\frac{\beta_{T_r} + T_r}{\beta + T} \right) \right] \right\}^{1/n_{BC}} \frac{\gamma_w}{\psi_{\text{aev}}} \ln\left[\left(1+\frac{q}{k_s}\right) e^{-\psi_{\text{aev}} z} - \frac{q}{k_s} \right] \left(\frac{\beta_{T_r} + T_r}{\beta + T} \right) \tag{22}$$

Eqs. (20) and (21) were developed based on the assumption that within the temperature range examined, the effect of temperature on the interface shear strength is controlled by thermally induced changes in apparent cohesion and that temperature has a negligible effect on the interface friction angle. The latter is consistent with the trends reported by most experimental test results in which the temperature is shown to have minimal effects on the effective angle of friction at critical state (e.g., Hueckel et al. 1998; Graham et al. 2001; Li et al. 2019).

Using the temperature-dependent matric suction and effective degree of saturation profiles introduced in the previous sections, the temperature-dependent model for the ultimate bearing capacity of an energy pile in unsaturated soils under drained conditions can be written as

$$\begin{aligned} Q_{(\text{unsat})} = & \left[c'_{a,T} + \beta_c \left(\sigma - u_a + \frac{\gamma_w}{\psi_{\text{aev}}} \ln\left[\left(1+\frac{q}{k_s}\right) e^{-\psi_{aev} z} - \frac{q}{k_s} \right] \left(\frac{\beta_{T_r} + T_r}{\beta + T} \right) \left\{ \exp\left[\ln\left[\left(1+\frac{q}{k_s}\right) e^{-\psi_{\text{aev}} z} - \frac{q}{k_s} \right] \left(\frac{\beta_{T_r} + T_r}{\beta + T} \right) \right] \right\}^{1/n_{BC}} \right) \right] \pi D L \\ & + \left[c'_{a,T} + N_c \left(\sigma - u_a + \frac{\gamma_w}{\psi_{\text{aev}}} \ln\left[\left(1+\frac{q}{k_s}\right) e^{-\psi_{\text{aev}} z} - \frac{q}{k_s} \right] \left(\frac{\beta_{T_r} + T_r}{\beta + T} \right) \left\{ \exp\left[\ln\left[\left(1+\frac{q}{k_s}\right) e^{-\psi_{\text{aev}} z} - \frac{q}{k_s} \right] \left(\frac{\beta_{T_r} + T_r}{\beta + T} \right) \right] \right\}^{1/n_{BC}} \right) \right] \frac{\pi D^2}{4} \end{aligned} \tag{23}$$

The first term in Eq. (23) represents the pile shaft capacity contribution, and the second term represents the pile end bearing capacity contribution. Table 1 gives soil specific parameters and relevant laboratory tests for saturated and unsaturated conditions. The rest of the parameters (σ_v, q, N_c, z, γ_w, L, D) are soil independent parameters. Compared to more conventional formulations (e.g., for fully saturated conditions), the only added parameters are those for the temperature-dependent SWRC. Eq. (23) offers a unified approach to estimate the ultimate bearing capacity of energy piles under varying temperatures and vertical flow rates in an unsaturated soil layer.

Model Validation

As noted, limited experimental data is available on the ultimate bearing capacity of energy piles in unsaturated soils under different temperatures. Accordingly, only the data from centrifuge tests performed by Goode and McCartney (2015) are used to validate the proposed model. Goode and McCartney (2015) measured the load-settlement curves of a semifloating energy pile having a prototype length of 8.2 m and prototype diameter of 1.5 m embedded in a layer of unsaturated Bonny silt for pile temperatures of 21°C, 32°C, and 40°C. Dielectric sensors were used to measure the temperature and the volumetric water content of the soil at a depth of 5.5 m below the pile tip and at a radial distance of 0.6 m from the soil–pile interface, and these results were presented in a follow-up study by Behbehani and McCartney (2020a). As the tests of Goode and McCartney (2015) were performed in compacted soil having a uniform initial suction with depth, Eq. (23) was used to evaluate the ultimate bearing capacity under no-flow conditions ($q = 0$) and constant suction and effective saturation with a depth corresponding to the different temperatures. Specifically, the effects of temperature on the suction and effective saturation were estimated using Eqs. (14) and (15), then were incorporated into Eq. (19).

To use the proposed model, we first determined the degree of saturation and the corresponding matric suction at different temperatures using the proposed formulations and compared them against the measured data. Table 2 presents the SWRC parameters used in the calculations. The SWRC parameters given in Table 2 were obtained by fitting the measured data at the reference temperature ($T = 21$°C). Fig. 1(a) shows the predicted SWRCs at different temperatures for Bonny silt. Applying a higher temperature causes the SWRC to shift downward. This means that by increasing the temperature at a given effective saturation, the matric suction will decrease, and at a given matric suction, the effective saturation decreases. The predicted temperature-dependent SWRC models were validated against laboratory measured data in Vahedifard et al. (2018, 2019).

A good match is observed between the measured and predicted values of the volumetric water content of unsaturated Bonny silt versus the change in temperature at a prototype distance from the pile of 0.6 m as shown in Fig. 2. The increase in temperature at this location caused a decrease in the volumetric water content of unsaturated silt. The good match in Fig. 2 indicates that the temperature-dependent SWRC may be sufficient to estimate the amount of thermally induced drying in the soil at equilibrium, without having to use a complex transient coupled heat transfer and water flow analysis like the one used by Behbehani and McCartney (2020a). In the next step, the input parameters given in Table 2 were used to calibrate the ultimate bearing capacity at the reference temperature (i.e., 21°C). The total stress at midheight of the pile was considered to be 75 kPa at prototype scale. The calibration process was performed by optimizing the β_c value, leading to the minimum

Table 1. Soil parameters used in the proposed formulation

Soil condition	Property	Parameter(s)	Relevant tests
Saturated	Shear strength parameters	$c'_{a,T}$, β_c	Conventional shear strength tests
	Intrinsic permeability	k_{in}	Permeability tests
Unsaturated	SWRC parameters	n_{BC}, ψ_{aev}	Water retention tests
	Enthalpy of immersion	Δh_{T_r}	Calorimetric test

Table 2. Input parameters for validation and parametric study

Soil	n_{BC}	ψ_{aev} (kPa)	Δh_{T_r} (J/m^2)	β_c	k_{in} (m^2)	$c'_{a,T}$ (kPa)
Bonny silt	0.37	19	−0.45	0.26	1×10^{-14}	0.0
Denver bentonite	0.27	100		0.25	1×10^{-16}	10.0

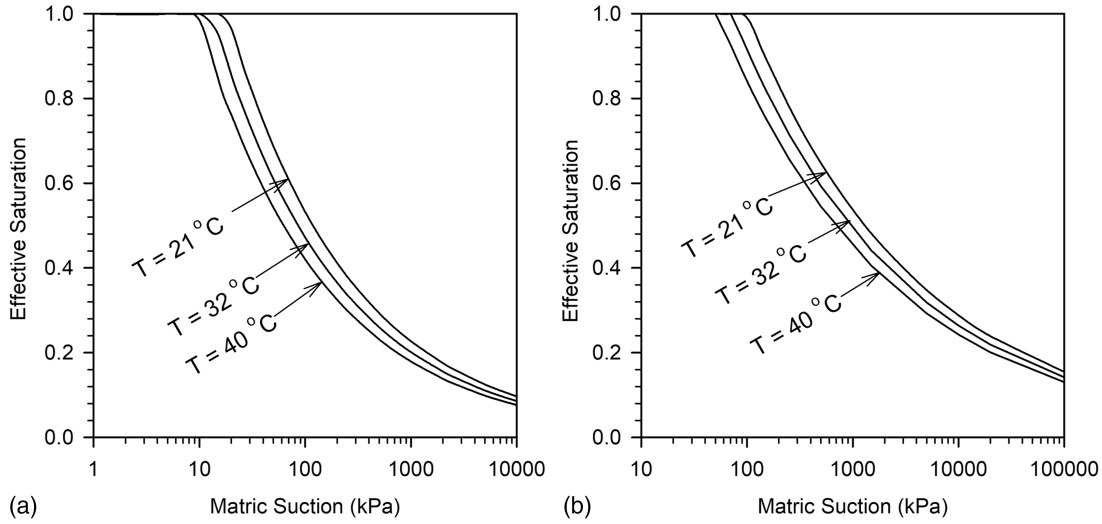

Fig. 1. Temperature-dependent SWRCs for (a) Bonny silt; and (b) Denver bentonite.

prediction error against the measured ultimate bearing capacity at 21°C. The calibrated model was then used with no further fitting to predict the ultimate bearing capacities at higher temperatures at the soil–pile interface (32°C and 40°C).

Fig. 3 depicts the predicted shaft capacity [Fig. 3(a)], the predicted end bearing capacity [Fig. 3(b)], and the measured and predicted ultimate bearing capacity [Fig. 3(c)]. As shown in Fig. 3(c), a good match is observed between the measured and predicted values of the ultimate bearing capacity of the energy pile in unsaturated Bonny silt versus the change in temperature from room temperature. The comparison shows a good agreement between the measured and predicted values. The increase in temperature at the soil–pile interface causes an increase in the ultimate bearing capacity of the energy pile in unsaturated silt. While the results show a very small error, the proposed model can benefit from further validation from instrumented energy piles in unsaturated soils.

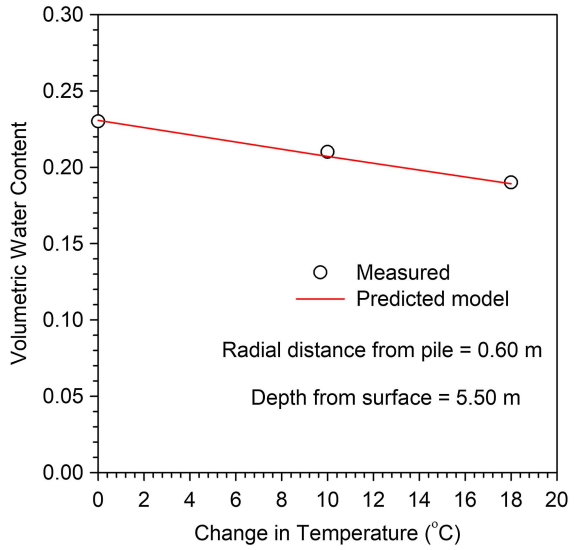

Fig. 2. Comparison between predicted versus measured volumetric water content in unsaturated Bonny silt with the measured change in temperature from ambient condition to elevated temperature. (Data from Behbehani and McCartney 2020a.)

Parametric Study

The proposed framework was employed in a parametric study to evaluate the effect of flow rate and aspect ratio on the ultimate bearing capacity of energy piles in unsaturated clay and silt subject to temperatures ranging from 5°C to 45°C. Table 2 and Fig. 1 present the input parameters and the SWRCs, respectively, of Denver bentonite and Bonny silt, which were used in the parametric study. In all cases, the water table was assumed to be at a depth of 20 m below the ground surface. Aspect ratio, AR, is defined as the ratio of the pile embedment length, L, to the pile diameter, D.

Effect of Flow Rate

Three flow rates were examined for each soil: $q = 0$ (hydrostatic), $q = -1.6 \times 10^{-9}$ m/s (infiltration), and $q = -3.0 \times 10^{-9}$ m/s (infiltration) for Denver bentonite; and $q = 0$ (hydrostatic), $q = -3.2 \times 10^{-8}$ m/s (infiltration), and -6.0×10^{-8} m/s (infiltration) for Bonny silt. The flow rates were chosen in such a way that q/k_s at the reference temperature varies between two extreme flow rates (i.e., 0.0 and −0.95) for each soil.

Fig. 4 shows the effective saturation, matric suction, and effective stress of Denver bentonite (hereafter referred to as clay) along the pile embedment length at different temperatures and flow rates. For a given pile length, the effective saturation decreases [Fig. 4(a)], and matric suction increases [Fig. 4(b)] with an increase in temperature from 5°C to 25°C and 45°C. At a given temperature, the effective saturation [Fig. 4(a)] and matric suction [Fig. 4(b)] monotonically change with pile length. On the other hand, the changes in effective stress [Fig. 4(c)] are monotonic at 5°C and 25°C and nonmonotonic at 45°C. The distinct variation of the properties is mainly due to thermally induced drying and liquid flow in the soil along the pile length. At any given length, as the flow rate changes from hydrostatic to infiltration state, the effective saturation increases and matric suction decreases with an increase in temperature.

Depending on the length of the pile and the effective saturation, the effective stress increases or decreases with temperature. Approximately up to 12 m depth from the ground surface, the effective stress increases, and from 12 m to the water table, the effective stress decreases at 45°C. At the other temperatures (5°C and 25°C), the effective stress increases at all pile lengths. As seen

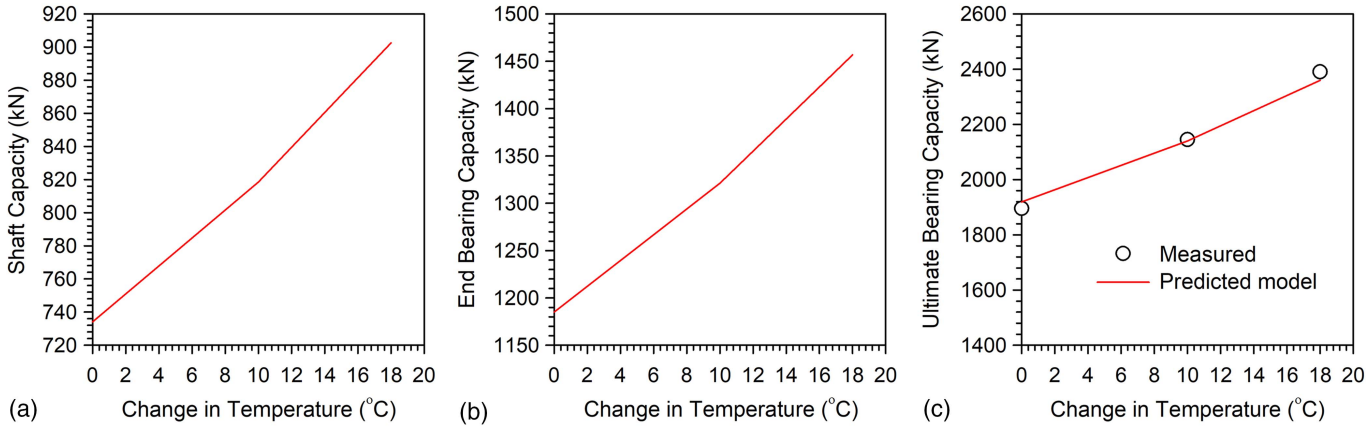

Fig. 3. Energy pile capacities with temperature: (a) predicted shaft capacity; (b) predicted end bearing capacity; and (c) measured and predicted ultimate bearing capacity. (Measured values from Behbehani and McCartney 2020a.)

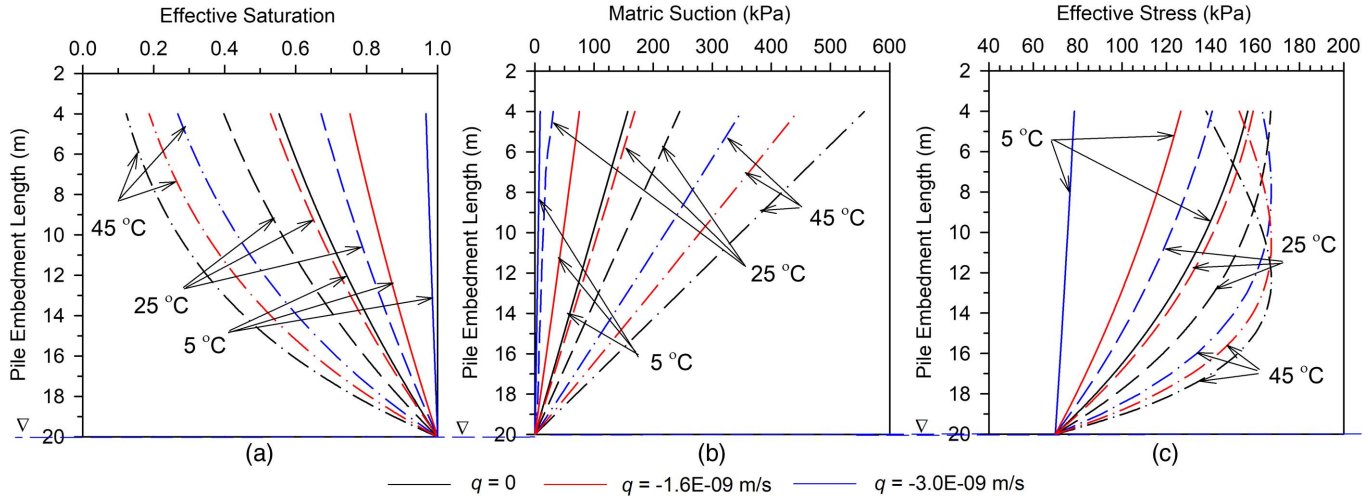

Fig. 4. Profiles along the pile embedment length in Denver bentonite at three temperatures and three flow rates: (a) effective saturation; (b) matric suction; and (c) effective stress.

in Fig. 4, the effective stress varies nonmonotonically at 45°C. After 12 m from the water table, there is a decrease in the effective stress. The degree of saturation at this depth is less than 0.3, which corresponds to the saturation level where the soil is transitioning from the funicular regime (continuous water state) to the pendular regime (discontinuous water state). This transition point can be referred to as the funicular water content (Thota et al. 2021; Cao et al. 2021). For ambient conditions, the effective stress trend is monotonic because the soil is still in the funicular regime and has not entered the pendular regime through depth yet. For ambient conditions, generally, at low degrees of saturation (near pendular) the rate of drying is slow but the rate of change in matric suction is not relatively slow. However, it is not the case at elevated temperatures. Therefore, there are reductions in suction stress (absolute value) and effective stress at 45°C.

At depths close to the water table (near saturation), the temperature has minimal effects on effective stress, whereas the temperature effect on effective stress increases as the distance from the water table increases. Thermally induced changes in effective stress can be attributed to the impact of temperature on physiochemical mechanisms of the porous medium, changing effective saturation, and matric suction under different flow conditions. At the water table, because the soil is in a saturated state, the flow rate has no effect on effective stress. It is important to note that the soil in this study is assumed to not deform significantly with changes in temperature, which would cause changes in the ultimate bearing capacity of the soil in saturated conditions (at the location of the water table). This assumption is reasonable for heavily overconsolidated low-plasticity soils, but the effects of volume change of saturated soils on the shaft capacity of energy piles have been observed in the literature (e.g., Ozudogru et al. 2015; Ravera et al. 2020).

Fig. 5 shows the variation of shaft capacity, end bearing capacity, and ultimate bearing capacity versus the pile embedment length for clay at temperatures of 5°C, 25°C, and 45°C under three flow rates with $AR = 10$. As shown in Fig. 5(a), for a given pile length, the shaft capacity increases with an increase in temperature and decreases as the flow rate changes from hydrostatic to infiltration for 5°C and 25°C and nonmonotonically varies at 45°C. For all flow rates, at the reference temperature, the shaft capacity monotonically

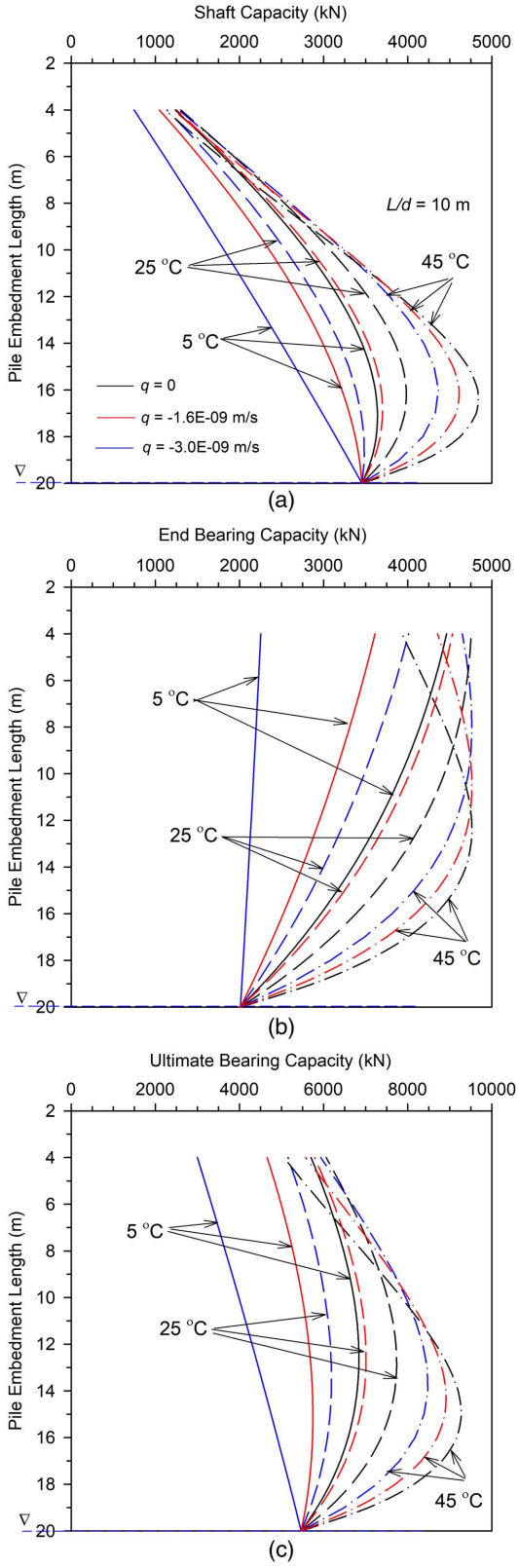

Fig. 5. Profiles versus embedment depth of pile in Denver bentonite at three temperatures and three flow rates: (a) shaft bearing capacity; (b) end bearing capacity; and (c) ultimate bearing capacity.

decreases with a decrease in the pile embedment length due to the reduction in the surface area available for mobilizing shaft capacity. However, at elevated temperatures, the variation of shaft capacity with the pile embedment length is nonmonotonic. First, the shaft capacity increases with greater pile embedment length, but after it reaches peak value, a decrease is observed with further increases in the pile embedment length. This could be due to the domination of changes in effective stress in piles with larger embedment lengths over the decrease in pile surface area available for shaft capacity mobilization. Beyond the peak value, with further increases of the pile embedment depth, the effects of the pile surface area available for side shear mobilization prevail over the effects of the effective stress on shaft capacity.

As shown in Fig. 5(b), for a given length, the end bearing capacity increases as the temperature increases from 5°C to 25°C and nonmonotonically varies at 45°C and decreases as the flow rate changes from 0 hydrostatic conditions to positive values (downward infiltration). The effect of temperature on the end bearing capacity increases as the pile embedment length decreases. This could be due to a lower variation of effective stress with the temperature near the water table and a higher variation of effective stress with temperature away from the water table. For all flow rates, at temperatures of 5°C and 25°C, the end bearing capacity monotonically increases. At 45°C, the end bearing capacity increases, reaches a peak, and then decreases with a decrease in the pile embedment length; overall, it follows the trend of effective stress.

Fig. 5(c) depicts that the temperature dependency of the ultimate bearing capacity of the pile in clay is controlled by thermally induced changes in the shaft and end bearing capacities. For a given pile embedment length, the ultimate bearing capacity increases with an increase in temperature from 5°C to 25°C and 45°C. For the reference temperature (5°C), the ultimate bearing capacity decreases monotonically with a decrease in the pile embedment length. At elevated temperatures (25°C and 45°C), similar to the trend of shaft capacity, the ultimate bearing capacity nonmonotonically varies with the pile embedment length. The percentage of increase in the ultimate bearing capacity by changing temperature increases as the flow rate changes from hydrostatic to infiltration. For example, at a depth of 12 m from the ground surface, the ultimate bearing capacity increases by approximately 13% and 27%, 24% and 53%, and 43% and 95%, by increasing the temperature from 5°C to 25°C and 45°C under flow rates of zero, -1.6×10^{-9} m/s, and -3.0×10^{-9} m/s, respectively. The increase in the ultimate bearing capacity of pile in clay with an increase in temperature can be attributed to the thermally induced reductions in the degree of saturation, which can increase matric suction in the soil surrounding the pile, thus increasing the apparent cohesion, effective stress, and the pile capacities at a given elevated temperature. The changes in effective saturation and matric suction with temperature are due to temperature-induced changes in the surface tension, contact angle, and wettability of soil (Grant and Salehzadeh 1996; Vahedifard et al. 2018, 2019).

Fig. 6 shows the effective saturation, matric suction, and effective stress of Bonny silt (hereafter referred to as silt) soil with the pile embedment length at temperatures of 5°C, 25°C, and 45°C under three flow rates of zero (hydrostatic), -3.2×10^{-8} m/s (infiltration), and -6.0×10^{-8} m/s (infiltration). Similar to the clay, for a given temperature, at different lengths, as we move from the saturated state to unsaturated state, the effective saturation decreases and matric suction increases. Unlike clay, however, two different trends were observed for effective stress along the pile length with temperature: (1) variation along the pile embedment length at a given temperature and (2) variation with the temperature at a given pile embedment length. First, the effective stress at the reference temperature increases monotonically, and at elevated temperatures it increases, reaches a peak, and decreases with further reduction in pile embedment length. Second, at depths close to the ground surface, the effective stress decreases, and at depths close to

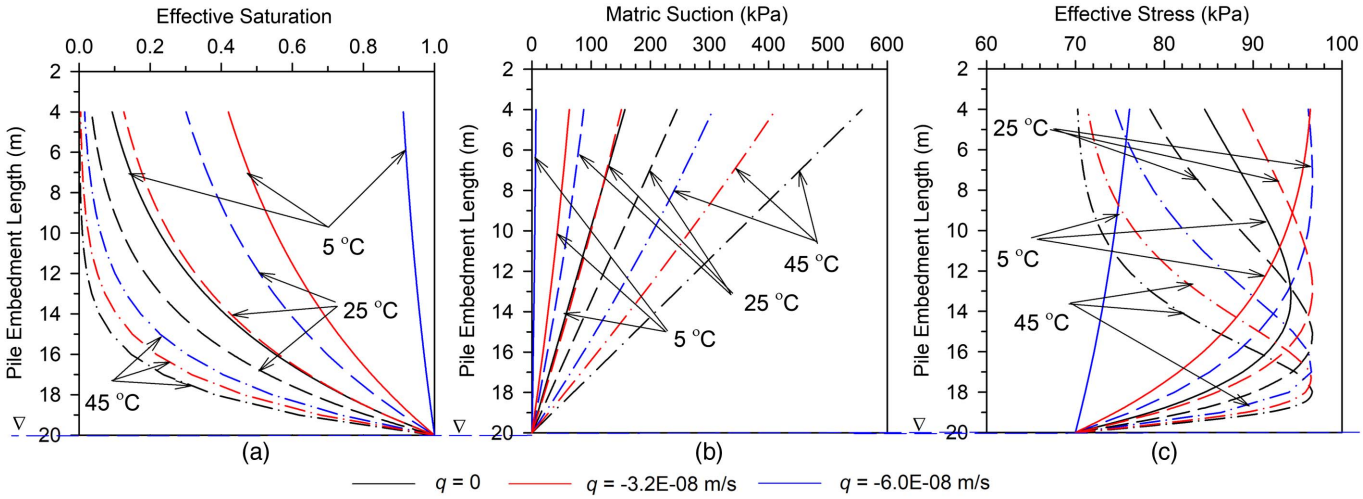

Fig. 6. Profiles along the pile embedment depth at the edge of the pile in Bonny silt at three temperatures and three flow rates: (a) effective saturation; (b) matric suction; and (c) effective stress.

the water table it increases with an increase in temperature. At relatively lower pile embedment lengths, the rate of thermally induced increase in effective stress is higher, whereas, at greater embedment lengths, the temperature has a less pronounced effect on effective stress. The trend at elevated temperatures is the same for all flow rates. Compared to clay (Fig. 4), there is a higher reduction in effective saturation with temperature in silt, which could be due to higher permeability and pore size characteristics for silt.

Fig. 7 shows the shaft capacity, end bearing capacity, and ultimate bearing capacity of the pile in unsaturated silt with pile embedment length at different temperatures and flow rates with $AR = 10$. The trends of the shaft, end bearing, and ultimate bearing capacities are different from clay. That is, the variations of shaft, end, and ultimate bearing capacities are monotonic at the reference temperature but become nonmonotonic (increase/decrease) under elevated temperatures with the pile embedment length. The behavior of pile capacities is mainly controlled by both effective stress and pile embedment length. The increase is due to the drying-induced increase of effective stress, and the transition to a decrease after attaining peak is due to wetting-induced reduction of effective stress. A similar type of transition (may be termed as a funicular water regime where the liquid water phase appears to be in a continuous state) occurs in unsaturated soil properties such as SWRC, thermal conductivity function, Poisson's ratio, and others. The range and variation of pile capacities along the pile embedment length are lower compared to clay. This distinct behavior could be due to the range of effective stress and hence apparent cohesion with temperature and pile length. For instance, at a depth of 12 m from the ground surface, the pile ultimate axial capacities vary by approximately 1% and 19%, −5% and −12%, and −29% and −18%, when increasing temperature from 5°C to 25°C and 45°C under flow rates of zero, -1.6×10^{-9} m/s, and -3.0×10^{-9} m/s, respectively. For elevated temperatures, the different flow rates have a similar effect on the ultimate bearing capacity.

Effect of Aspect Ratio

For each soil, three different aspect ratios were examined: $AR = 5$, 10, and 20. To isolate the effect of aspect ratio, the flow rate was kept to $q = 0$ (hydrostatic) in this section. Fig. 8 shows the variation of shaft capacity, end bearing capacity, and ultimate bearing capacity versus the pile embedment length for clay at temperatures of 5°C, 25°C, and 45°C and *AR*s of 5, 10, and 20. Because the suction, effective saturation, and effective stress profiles are independent of *AR*, they are the same as shown in Fig. 4 for the zero flow rate.

For all *AR*s, the shaft and ultimate bearing capacities of the pile in clay change nonmonotonically, and the end bearing capacity of the pile monotonically changes at a given temperature. The temperature dependency of the ultimate bearing capacity is less at the water table (near saturated state) and close to the ground surface. This can be interpreted as the effects of temperature on the pile capacity are the largest in the capillary regime of the SWRC. Further, the impact of temperature on the ultimate bearing capacity increases as *AR* decreases because of the higher surface area of the pile available for shaft capacity. For higher *AR*, the temperature has a minimal effect on ultimate bearing capacity. For instance, for a 12-m-long pile, the ultimate bearing capacity increases by approximately 13% and 27%, 13% and 28%, and 12% and 26%, by increasing the temperature from 5°C to 25°C and 45°C under *AR*s of 5, 10, and 20, respectively.

Fig. 9 shows the variation of the shaft, end bearing, and ultimate bearing capacities with pile embedment depths for silt at temperatures of 5°C, 25°C, and 45°C and *AR*s of 5, 10, and 20 under no-flow conditions. The suction, effective saturation, and effective stress profiles are the same as shown in Fig. 6 for the zero flow rate case. The shaft, end bearing, and ultimate bearing capacities nonmonotonically vary with temperature along the pile embedment length. For all temperatures, the shaft, end, and ultimate bearing capacities have a similar trend versus the pile embedment length. They first slightly increase close to the water table, reach a peak, and then decrease. Unlike clay, the percent increase in pile capacities with temperature in silt remains approximately the same for all *AR*s. For example, at a pile embedment length of 10 m, the pile capacities decrease between 4% and 21% by increasing the temperature from 5°C to 45°C regardless of *AR*s. On the other hand, at a specific pile embedment length, the variation of *AR*s is shown to have a higher impact on pile capacities compared to elevated changes in temperature.

Most of the existing studies focused on saturated state and neglected the unsaturated conditions. It is evident from the current study that, for $q = -3.0 \times 10^{-9}$ m/s, at a pile embedment depth

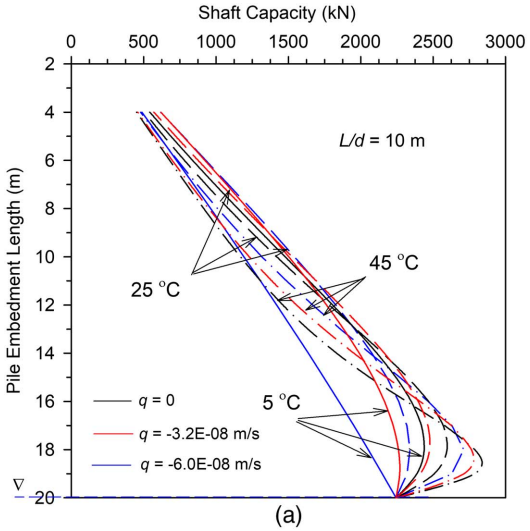

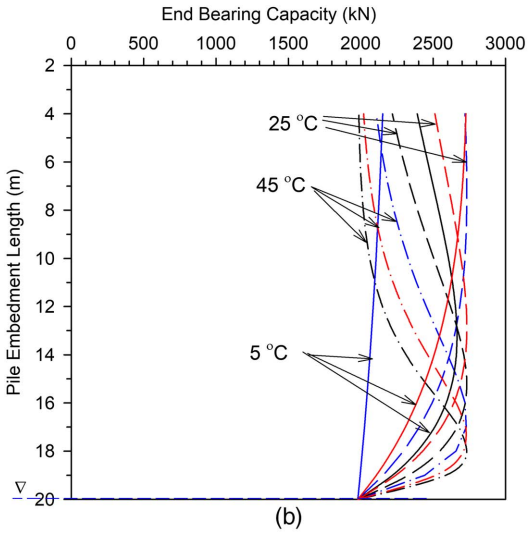

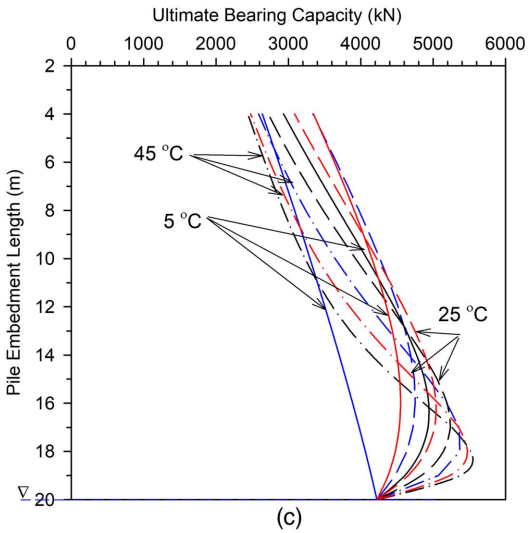

Fig. 7. Profiles versus embedment depth of pile in Bonny silt at three temperatures and three flow rates: (a) shaft bearing capacity; (b) end bearing capacity; and (c) ultimate bearing capacity.

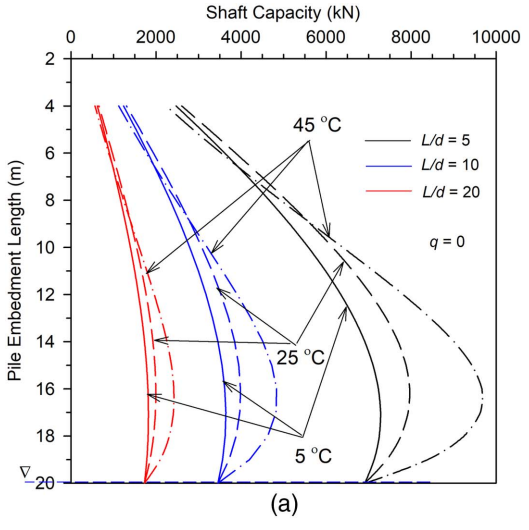

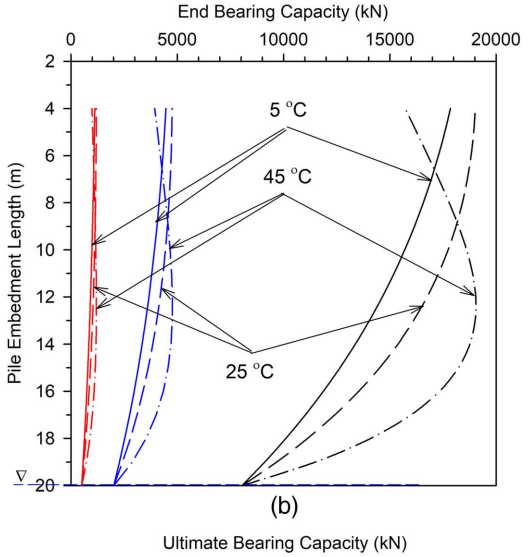

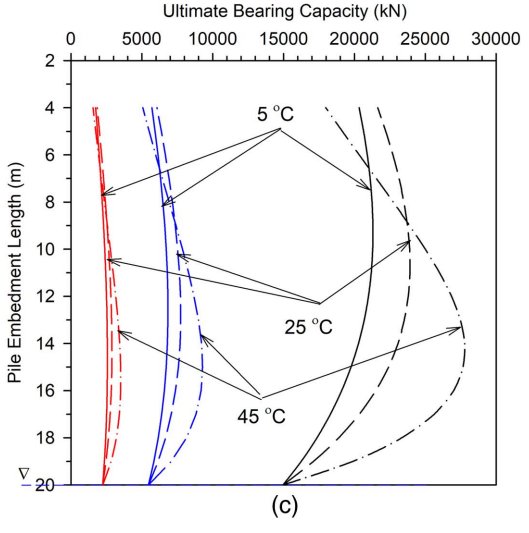

Fig. 8. Profiles versus embedment depth of pile in Denver bentonite at three temperatures and three aspect ratios: (a) shaft bearing capacity; (b) end bearing capacity; and (c) ultimate bearing capacity.

of 10 m, the ultimate bearing capacity of a pile in unsaturated clay ($S = 90\%$) changes by -27%, 9%, and 63% relative to the saturated conditions ($S = 100\%$) for temperatures of 5°C, 25°C, and 45°C, respectively. Similarly, for $q = -6.0 \times 10^{-8}$ m/s, at a pile embedment depth of 10 m, the ultimate bearing capacity of a pile in unsaturated silt ($S = 80\%$) varies by -20%, 4%, and 43% relative to saturated conditions ($S = 100\%$) for temperatures of 5°C, 25°C, and 45°C, respectively.

J. Geotech. Geoenviron. Eng., 2021, 147(11): 04021132

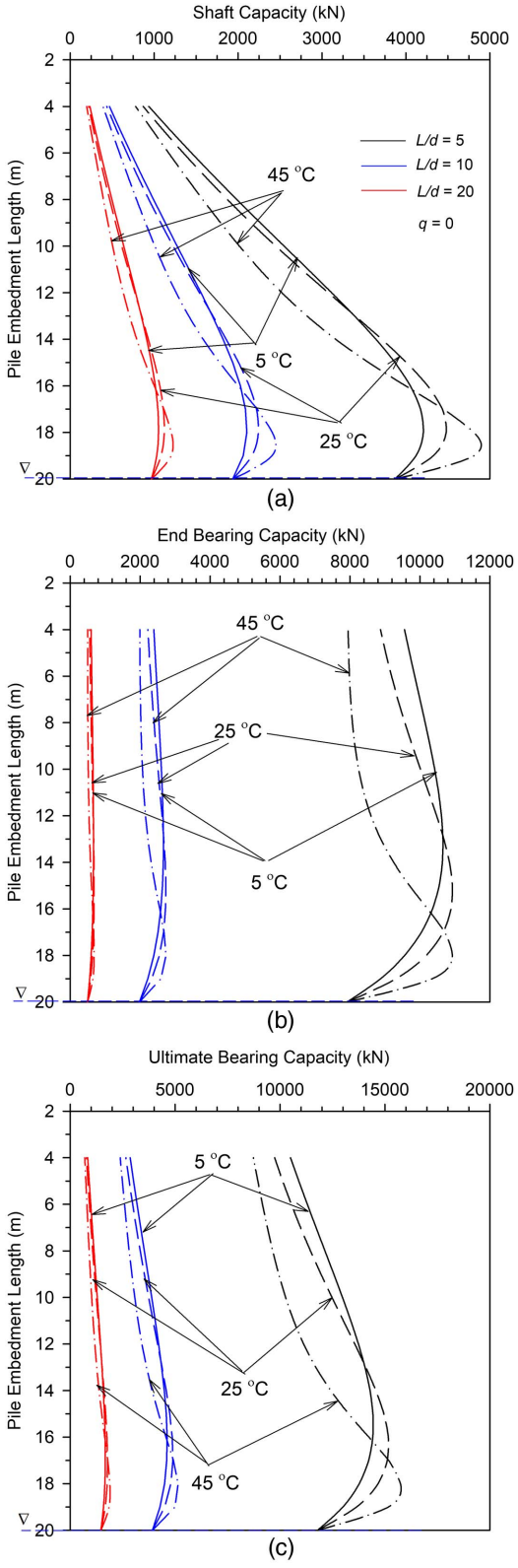

Fig. 9. Profiles versus embedment depth of pile in Bonny silt at three temperatures and three aspect ratios: (a) shaft bearing capacity; (b) end bearing capacity; and (c) ultimate bearing capacity.

Conclusions

This paper introduced an analytical model to estimate the ultimate bearing capacity of energy piles in unsaturated fine-grained soils under different temperatures and steady flow rates. For this purpose, the formulations for temperature-dependent matric suction and effective saturation were incorporated for calculating the shaft capacity, end bearing capacity, and ultimate bearing capacity of energy piles in unsaturated soils subject to different temperatures. To simplify the model, it was assumed that the soil did not change in volume with heating and that temperature effects on the matric suction and effective saturation were sufficient to capture the effects of thermally induced drying of unsaturated soils. The results of the proposed model were validated against one set of experimental data available in the literature. Further, to demonstrate the temperature dependency of the ultimate bearing capacity, a parametric study was conducted with clayey and silty soils at temperatures of 5°C, 25°C, and 45°C, three flow rates (one hydrostatic and two infiltrations), and three aspect ratios (5, 10, and 20). The results were presented in the form of shaft capacity, end bearing capacity, and ultimate bearing capacity along the embedment length of the pile.

The results suggested that temperature changes can have a notable effect on matric suction and effective saturation and thereby the ultimate bearing capacity of the pile. For clay, an increase in the effective stress and the ultimate pile bearing capacity is observed under elevated temperatures. For silt, at elevated temperatures, a nonmonotonic behavior of effective stress and hence the ultimate bearing capacity is noted. At a given temperature, for clay, the ultimate bearing capacity decreases, and for silt, it increases/decreases based on the pile embedment length, as the flow rate changes from hydrostatic to infiltration conditions. Further, the bearing capacity increases as the aspect ratio decreases.

The study highlighted the considerable impacts of temperature on parameters related to hydraulic conductivity and apparent cohesion of unsaturated soils that could control the ultimate bearing capacity of energy piles under elevated temperatures. The proposed analytical model provides an effective approach to estimate the ultimate bearing capacity of energy piles under various thermal and hydraulic loadings as part of a soil–structure interaction design process. Future studies are suggested to collect more experimental data of ultimate bearing capacity at various effective saturations under drained and undrained thermal, hydraulic, and mechanical loading cases. Such data can be employed to further validate the proposed model.

Data Availability Statement

All data, models, and code generated or used during the study appear in the published article.

Acknowledgments

This material is based upon work supported by the National Science Foundation under Grant No. CMMI-1634748. Any opinions, findings, and conclusions or recommendations expressed in this material are those of the authors and do not necessarily reflect the views of the National Science Foundation.

References

Akrouch, G. A., M. Sánchez, and J. L. Briaud. 2014. "Thermo-mechanical behavior of energy piles in high plasticity clays." *Acta Geotech.* 9 (3): 399–412. https://doi.org/10.1007/s11440-014-0312-5.

Akrouch, G. A., M. Sánchez, and J. L. Briaud. 2016. "An experimental, analytical and numerical study on the thermal efficiency of energy piles in unsaturated soils." *Comput. Geotech.* 71 (Jan): 207–220. https://doi.org/10.1016/j.compgeo.2015.08.009.

Başer, T., Y. Dong, A. M. Moradi, N. Lu, K. Smits, S. Ge, D. Tartakovsky, and J. S. McCartney. 2018. "Role of nonequilibrium water vapor diffusion in thermal energy storage systems in the vadose zone." *J. Geotech. Geoenviron. Eng.* 144 (7): 04018038. https://doi.org/10.1061/(ASCE)GT.1943-5606.0001910.

Behbehani, F., and J. S. McCartney. 2020a. "Impacts of unsaturated conditions on the ultimate axial capacity of energy piles." In Vol. 195 of *Proc., EUnsat 2020: The 4th European Conf. on Unsaturated Soils*, 04005. Les Ulis, France: EDP Sciences.

Behbehani, F., and J. S. McCartney. 2020b. "Simulation of the thermo-hydraulic response of energy piles in unsaturated soils." In Vol. 205 of *Proc., 2nd Int. Conf. on Energy Geotechnics (ICEGT-2020)*, 05002. Les Ulis, France: EDP Sciences.

Bishop, A. W. 1959. "The principle of effective stress." *Teknisk Ukeblad* 106 (39): 859–863.

Bourne-Webb, P. J., B. Amatya, K. Soga, T. Amis, C. Davidson, and P. Payne. 2009. "Energy pile test at Lambeth College, London: Geotechnical and thermodynamic aspects of pile response to heat cycles." *Géotechnique* 59 (3): 237–248. https://doi.org/10.1680/geot.2009.59.3.237.

Brandl, H. 2006. "Energy foundations and other thermo-active ground structures." *Géotechnique* 56 (2): 81–122. https://doi.org/10.1680/geot.2006.56.2.81.

Brooks, R. H., and A. T. Corey. 1964. *Hydraulic properties of porous media*. Hydrology Paper No. 3. Fort Collins, CO: Colorado State Univ.

Burland, J. B. 1973. "Shaft friction of piles in clay-a simple fundamental approach." *Ground Eng.* 6 (3): 30–42.

Campbell, G. S., J. D. Jungbauer Jr., W. R. Bidlake, and R. D. Hungerford. 1994. "Predicting the effect of temperature on soil thermal conductivity." *Soil Sci.* 158 (5): 307–313. https://doi.org/10.1097/00010694-199411000-00001.

Cao, T. C., S. K. Thota, F. Vahedifard, and A. Amirlatifi. 2021. "A temperature-dependent model for thermal conductivity function of unsaturated soils." In *Proc., 2021 Int. Foundations Congress and Equipment Exposition, IFCEE 2021*, 89–98. Reston, VA: ASCE. https://doi.org/10.1061/9780784483428.010.

Chandler, R. J. 1968. "The shaft friction of piles in cohesive soils in terms of effective stress." *Civ. Eng. Public Works Rev.* 60 (708): 48–51.

Chen, D., and J. S. McCartney. 2017. "Parameters for load transfer analysis of energy piles in uniform nonplastic soils." *Int. J. Geomech.* 17 (7): 04016159. https://doi.org/10.1061/(ASCE)GM.1943-5622.0000873.

Constantz, J. 1982. "Temperature dependence of unsaturated hydraulic conductivity of two soils." *Soil Sci. Soc. Am. J.* 46 (3): 466–470. https://doi.org/10.2136/sssaj1982.03615995004600030005x.

Di Donna, A., A. Ferrari, and L. Laloui. 2016a. "Experimental investigations of the soil–concrete interface: Physical mechanisms, cyclic mobilization, and behaviour at different temperatures." *Can. Geotech. J.* 53 (4): 659–672. https://doi.org/10.1139/cgj-2015-0294.

Di Donna, A., and L. Laloui. 2013. "Soil response under thermomechanical conditions imposed by energy geostructures." In *Energy geostructures: Innovation in underground engineering*, 3–21. Hoboken, NJ: Wiley.

Di Donna, A., A. F. R. Loria, and L. Laloui. 2016b. "Numerical study of the response of a group of energy piles under different combinations of thermo-mechanical loads." *Comput. Geotech.* 72 (Feb): 126–142. https://doi.org/10.1016/j.compgeo.2015.11.010.

Dorsey, N. E. 1940. *Properties of ordinary water substance*. New York: Reinhold.

Elzeiny, R., M. T. Suleiman, S. Xiao, M. A. A. Qamar, and M. Al-Khawaja. 2020. "Laboratory-scale pull-out tests on a geothermal energy pile in dry sand subjected to heating cycles." *Can. Geotech. J.* 57 (11): 1754–1766. https://doi.org/10.1139/cgj-2019-0143.

Fu, Z. 2017. "Thermo-hydro-mechanical effects on the behaviour of unsaturated soil-structure interfaces and the numerical analysis of energy piles." Ph.D. dissertation, Dept. of Civil Engineering, Univ. of Ottawa.

Fuentes, R., N. Pinyol, and E. Alonso. 2016. "Effect of temperature induced excess porewater pressures on the shaft bearing capacity of geothermal piles." *Geomech. Energy Environ.* 8 (Dec): 30–37. https://doi.org/10.1016/j.gete.2016.10.003.

Gardner, W. R. 1958. "Some steady-state solutions of the unsaturated moisture flow equation with application to evaporation from a water table." *Soil Sci.* 85 (4): 228–232. https://doi.org/10.1097/00010694-195804000-00006.

Georgiadis, K., D. M. Potts, and L. Zdravkovic. 2003. "The influence of partial soil saturation on pile behaviour." *Géotechnique* 53 (1): 11–25. https://doi.org/10.1680/geot.2003.53.1.11.

Goode, J. C., III, and J. S. McCartney. 2015. "Centrifuge modeling of end-restraint effects in energy foundations." *J. Geotech. Geoenviron. Eng.* 141 (8): 04015034. https://doi.org/10.1061/(ASCE)GT.1943-5606.0001333.

Graham, J., N. Tanaka, T. Crilly, and M. Alfaro. 2001. "Modified Cam-clay modelling of temperature effects in clays." *Can. Geotech. J.* 38 (3): 608–621. https://doi.org/10.1139/t00-125.

Grant, S. A. 2003. "Extension of temperature effects model for capillary pressure saturation relations." *Water Resour. Res.* 39 (1): SBH 1–SBH 10. https://doi.org/10.1029/2000WR000193.

Grant, S. A., and A. Salehzadeh. 1996. "Calculation of temperature effects on wetting coefficients of porous solids and their capillary pressure functions." *Water Resour. Res.* 32 (2): 261–270. https://doi.org/10.1029/95WR02915.

Haar, L., J. S. Gallagher, and G. S. Kell. 1984. *NBS/NRC steam table*. New York: Hemisphere Publishing Corporation.

Hueckel, T., R. Pellegrini, and C. Del Olmo. 1998. "A constitutive study of thermo-elasto-plasticity of deep carbonatic clays." *Int. J. Numer. Anal. Methods Geomech.* 22 (7): 549–574. https://doi.org/10.1002/(SICI)1096-9853(199807)22:7<549::AID-NAG927>3.0.CO;2-R.

Kalantidou, A., A. M. Tang, J. Pereira, and G. Hassen. 2012. "Preliminary study on the mechanical behaviour of heat exchanger pile in physical model." *Géotechnique* 62 (11): 1047–1051. https://doi.org/10.1680/geot.11.T.013.

Knellwolf, C., H. Peron, and L. Laloui. 2011. "Geotechnical analysis of heat exchanger piles." *J. Geotech. Geoenviron. Eng.* 137 (10): 890–902. https://doi.org/10.1061/(ASCE)GT.1943-5606.0000513.

Kramer, C. A., and P. Basu. 2014. "Performance of a model geothermal pile in sand." In *Proc., 8th Int. Conf. on Physical Modelling in Geotechnics*, edited by C. Gaudin and D. White, 771–777. Leiden, Netherlands: CRC Press/Balkema.

Laloui, L., and A. F. R. Loria. 2019. *Analysis and design of energy geostructures: Theoretical essentials and practical application*. London: Academic Press.

Laloui, L., M. Nuth, and L. Vulliet. 2006. "Experimental and numerical investigations of the behaviour of a heat exchanger pile." *Int. J. Numer. Anal. Methods Geomech.* 30 (8): 763–781. https://doi.org/10.1002/nag.499.

Li, C., G. Kong, H. Liu, and H. Abuel-Naga. 2019. "Effect of temperature on behaviour of red clay–structure interface." *Can. Geotech. J.* 56 (1): 126–134. https://doi.org/10.1139/cgj-2017-0310.

Lide, D. R. 1995. *Handbook of chemistry and physics*. 75th ed. New York: CRC Press.

Liu, H. L., C. L. Wang, G. Q. Kong, and A. Bouazza. 2019. "Ultimate bearing capacity of energy piles in dry and saturated sand." *Acta Geotech.* 14 (3): 869–879. https://doi.org/10.1007/s11440-018-0661-6.

Loria, A. F. R., A. Gunawan, C. Shi, L. Laloui, and C. W. W. Ng. 2015. "Numerical modelling of energy piles in saturated sand subjected to thermo-mechanical loads." *Geomech. Energy Environ.* 1 (Apr): 1–15. https://doi.org/10.1016/j.gete.2015.03.002.

Loveridge, F. A., G. Narsilio, M. Sánchez, and J. S. McCartney. 2019. "Energy geostructures: A review of analysis approaches, in situ testing and model scale experiments." *Geomech. Energy Environ.* 22 (May): 100173. https://doi.org/10.1016/j.gete.2019.100173.

Lu, N., and Y. Dong. 2015. "Closed-form equation for thermal conductivity of unsaturated soils at room temperature." *J. Geotech. Geoenviron. Eng.* 141 (6): 04015016. https://doi.org/10.1061/(ASCE)GT.1943-5606.0001295.

Lu, N., J. W. Godt, and D. T. Wu. 2010. "A closed-form equation for effective stress in unsaturated soil." *Water Resour. Res.* 46 (5): 1–14. https://doi.org/10.1029/2009WR008646.

Lu, N., and D. V. Griffiths. 2004. "Profiles of steady-state suction stress in unsaturated soils." *J. Geotech. Geoenviron. Eng.* 130 (10): 1063–1076. https://doi.org/10.1061/(ASCE)1090-0241(2004)130:10(1063).

McCartney, J. S., N. H. Jafari, T. Hueckel, M. Sanchez, and F. Vahedifard. 2019. "Emerging thermal issues in geotechnical engineering." In *Geotechnical fundamentals for addressing new world challenges*, edited by N. Lu and J. K. Mitchell, 275–317. Cham, Switzerland: Springer. https://doi.org/10.1007/978-3-030-06249-1_10.

McCartney, J. S., and K. D. Murphy. 2017. "Investigation of potential dragdown/uplift effects on energy piles." *Geomech. Energy Environ.* 10 (Jun): 21–28. https://doi.org/10.1016/j.gete.2017.03.001.

McCartney, J. S., and J. E. Rosenberg. 2011. "Impact of heat exchange on side shear in thermo-active foundations." In *Geo-Frontiers 2011: Advances in Geotechnical Engineering*, 488–498. Reston, VA: ASCE.

Murphy, K. D., and J. S. McCartney. 2014. "Thermal borehole shear device." *ASTM Geotech. Test. J.* 37 (6): 1040–1055. https://doi.org/10.1520/GTJ20140009.

Murphy, K. D., J. S. McCartney, and K. S. Henry. 2015. "Evaluation of thermo-mechanical and thermal behavior of full-scale energy foundations." *Acta Geotech.* 10 (2): 179–195. https://doi.org/10.1007/s11440-013-0298-4.

Ng, C. W. W., C. Shi, A. Gunawan, L. Laloui, and H. L. Liu. 2015. "Centrifuge modelling of heating effects on energy pile performance in saturated sand." *Can. Geotech. J.* 52 (8): 1045–1057. https://doi.org/10.1139/cgj-2014-0301.

Olgun, C. G., T. Y. Ozudogru, S. L. Abdelaziz, and A. Senol. 2015. "Long-term performance of heat exchanger piles." *Acta Geotech.* 10 (5): 553–569. https://doi.org/10.1007/s11440-014-0334-z.

Ozudogru, T. Y., C. G. Olgun, and C. F. Arson. 2015. "Analysis of friction induced thermo-mechanical stresses on a heat exchanger pile in isothermal soil." *Geotech. Geol. Eng.* 33 (2): 357–371. https://doi.org/10.1007/s10706-014-9821-0.

Philip, J. R. 1969. "Theory of infiltration." In Vol. 5 of *Advances in hydroscience*, 215–296. Amsterdam, Netherlands: Elsevier.

Philip, J. R., and D. A. De Vries. 1957. "Moisture movement in porous materials under temperature gradients." *EOS, Trans. Am. Geophys. Union* 38 (2): 222–232. https://doi.org/10.1029/TR038i002p00222.

Pillsbury, A. F. 1950. "Effects of particle size and temperature on the permeability of sand to water." *Soil Sci.* 70 (4): 299–300. https://doi.org/10.1097/00010694-195010000-00005.

Ravera, E., M. Sutman, and L. Laloui. 2020. "Load transfer method for energy piles in a group with pile–soil–slab–pile interaction." *J. Geotech. Geoenviron. Eng.* 146 (6): 04020042. https://doi.org/10.1061/(ASCE)GT.1943-5606.0002258.

Saggu, R., and T. Chakraborty. 2015. "Cyclic thermo-mechanical analysis of energy piles in sand." *Geotech. Geol. Eng.* 33 (2): 321–342. https://doi.org/10.1007/s10706-014-9798-8.

Skempton, A. W. 1959. "Cast in-situ bored piles in London clay." *Géotechnique* 9 (4): 153–173. https://doi.org/10.1680/geot.1959.9.4.153.

Suryatriyastuti, M. E., H. Mroueh, and S. Burlon. 2013. "Numerical analysis of the bearing capacity of thermoactive piles under cyclic axial loading." Chap. 7 in *Energy geostructures: Innovation in underground engineering*, edited by L. Laloui and A. Di Donna. Hoboken, NJ: Wiley.

Suryatriyastuti, M. E., H. Mroueh, and S. Burlon. 2014. "A load transfer approach for studying the cyclic behavior of thermo-active piles." *Comput. Geotech.* 55 (Jan): 378–391. https://doi.org/10.1016/j.compgeo.2013.09.021.

Thota, S. K. 2020. "Temperature effects on unsaturated soils: Constitutive relationships and emerging geotechnical applications." Ph.D. dissertation, Dept. of Civil and Environmental Engineering, Mississippi State Univ.

Thota, S. K., T. C. Cao, and F. Vahedifard. 2021. "Poisson's ratio characteristic curve of unsaturated soils." *J. Geotech. Geoenviron. Eng.* 147 (1): 04020149. https://doi.org/10.1061/(ASCE)GT.1943-5606.0002424.

Thota, S. K., T. D. Cao, F. Vahedifard, and E. Ghazanfari. 2019. "Stability analysis of an unsaturated silty slope under nonisothermal conditions." In *Proc., Geo-Congress 2019: Geotechnical Materials, Modeling, and Testing*, 844–852. Reston, VA: ASCE. https://doi.org/10.1061/9780784482124.085.

Thota, S. K., and F. Vahedifard. 2020. "A model for ultimate bearing capacity of piles in unsaturated soils under elevated temperatures." In Vol. 205 of *Proc., E3S Web of Conf.*, 05003. Les Ulis, France: EDP Sciences. https://doi.org/10.1051/e3sconf/202020505003.

Thota, S. K., and F. Vahedifard. 2021. "Stability analysis of unsaturated slopes under elevated temperatures." *Eng. Geol.* 294: 106317. https://doi.org/10.1016/j.enggeo.2021.106317.

Uchaipichat, A. 2005. "Experimental investigation and constitutive modelling of thermo-hydro-mechanical coupling in unsaturated soils." Ph.D. thesis, School of Civil and Environmental Engineering, Univ. of New South Wales.

Uchaipichat, A. 2012. "Variation of pile capacity in unsaturated clay layer with suction." *Electron. J. Geotech. Eng.* 17: 2425–2433.

Uchaipichat, A. 2013. "Pile capacity in silt layer under elevated temperature." *Electron. J. Geotech. Eng.* 18: 5499–5505.

Vahedifard, F., T. D. Cao, E. Ghazanfari, and S. K. Thota. 2019. "Closed-form models for nonisothermal effective stress of unsaturated soils." *J. Geotech. Geoenviron. Eng.* 145 (9): 04019053. https://doi.org/10.1061/(ASCE)GT.1943-5606.0002094.

Vahedifard, F., T. D. Cao, S. K. Thota, and E. Ghazanfari. 2018. "Nonisothermal models for soil–water retention curve." *J. Geotech. Geoenviron. Eng.* 144 (9): 04018061. https://doi.org/10.1061/(ASCE)GT.1943-5606.0001939.

Vahedifard, F., D. Leshchinsky, K. Mortezaei, and N. Lu. 2016. "Effective stress-based limit equilibrium analysis for homogeneous unsaturated slopes." *Int. J. Geomech.* 16 (6): D4016003. https://doi.org/10.1061/(ASCE)GM.1943-5622.0000554.

Vahedifard, F., S. K. Thota, T. D. Cao, R. A. Samarakoon, and J. S. McCartney. 2020. "A temperature-dependent model for small-strain shear modulus of unsaturated soils." *J. Geotech. Geoenviron. Eng.* 146 (12): 04020136. https://doi.org/10.1061/(ASCE)GT.1943-5606.0002406.

Vanapalli, S. K., and Z. N. Taylan. 2012. "Design of single piles using the mechanics of unsaturated soils." *Int. J. GEOMATE* 2 (1): 197–204.

Vasilescu, A. R., A. L. Fauchille, C. Dano, P. Kotronis, R. Manirakiza, and P. Gotteland. 2019. "Impact of temperature cycles at soil–concrete interface for energy piles." In *Proc., Int. Symp. on Energy Geotechnics*, 35–42. Cham, Switzerland: Springer.

Wang, B., A. Bouazza, D. Barry-Macaulay, M. R. Singh, M. Webster, C. Haberfield, and S. Baycan. 2012. "Field and laboratory investigation of a heat exchanger pile." In *Proc., GeoCongress 2012: State of the Art and Practice in Geotechnical Engineering*, 4396–4405. Reston, VA: ASCE.

Wang, W., R. A. Regueiro, and J. S. McCartney. 2015. "Coupled axisymmetric thermo-poro-mechanical finite element analysis of energy foundation centrifuge experiments in partially saturated silt." *Geotech. Geol. Eng.* 33 (2): 373–388. https://doi.org/10.1007/s10706-014-9801-4.

Watson, K. M. 1943. "Thermodynamics of the liquid state." *Ind. Eng. Chem.* 35 (4): 398–406. https://doi.org/10.1021/ie50400a004.

Xiao, S., M. T. Suleiman, and J. S. McCartney. 2014. "Shear behavior of silty soil and soil-structure interface under temperature effects." In *Proc., Geo-Congress 2014: Geo-characterization and Modeling for Sustainability*, 4105–4114. Reston, VA: ASCE.

Yavari, N., A. M. Tang, J. M. Pereira, and G. Hassen. 2016. "Effect of temperature on the shear strength of soils and the soil–structure interface." *Can. Geotech. J.* 53 (7): 1186–1194. https://doi.org/10.1139/cgj-2015-0355.

Yazdani, S., S. Helwany, and G. Olgun. 2019. "Influence of temperature on soil–pile interface shear strength." *Geomech. Energy Environ.* 18 (Jun): 69–78. https://doi.org/10.1016/j.gete.2018.08.001.